Young's Modulus Evaluation of the Walls of Cerebral Arteries with Aneurysms

Frolov S.V.
Department of Biomedical Engineering
Tambov State Technical University
Tambov, Russia
sergej.frolov@gmail.com

Potlov A.Yu.
Department of Biomedical Engineering
Tambov State Technical University
Tambov, Russia
zerner@yandex.ru

Proskurin S.G.
Department of Biomedical Engineering
Tambov State Technical University
Tambov, Russia
spros@tamb.ru

Frolova T.A.
Department of Biomedical Engineering
Tambov State Technical University
Tambov, Russia
frolova2000@gmail.com

***Abstract* — A method for *in vivo* evaluation the value of the modulus of longitudinal elasticity (Young's modulus) for the large blood vessel walls was described. Digital processing of a sequence of optical coherence tomography (OCT) structural images of the investigated blood vessels' walls is the key feature of the described method. The pulse wave is used as a physiological and therefore relatively safe deforming impact. The absolute displacement of the blood vessel wall structures is calculated from the shift of peaks in the averaged A-scan interferograms. The size of the deformable region in the structural OCT images and the deforming area are considered to be equal to the coherence probing depth and the scanning area of the intravascular probe, respectively. The described method is to be used for choosing the optimal flow-diverter for correct treatment of cerebral arteries with aneurysms.**

Keywords* — *optical coherence tomography; compression elastography; pulse wave; Young's modulus; aneurysms

I. Introduction

An aneurysm is a pathological local expansion of the lumen of a blood vessel due to stretching of its wall. A ruptured aneurysm (especially an aneurysm of the brain artery) could cause fatal cerebral hemorrhage, blood stroke. At least 3% of the adult population suffers from cerebral aneurysm according to the World Health Organization reference data. The most promising method for cerebral aneurysms treatment is the deployment of flow-diverter in the affected artery. However, deployment of a flow-diverter is a complicated minimally invasive surgical procedure, which has not only a therapeutic effect, but also essential risks and financial expenses. In this regard, the deployment of a flow-diverter into the cerebral artery is carried out only in a situation with a high probability of an aneurysm rupture. Correct assessment of the risk of cerebral aneurysm rupture is a complex scientific and technical problem. There are two main approaches to solve this problem.

The first, uses methods for assessing the risk of aneurysm rupture based on analysis of aneurysm geometry and additional risk factors (high blood pressure, diabetes, smoking, etc.) These methods widely used in real clinical practice but it lead to contradictory results due to a simplified approach to the problem.

The second approach, consists of the methods for assessing the risk of aneurysm rupture based on individualized numerical simulation of cerebral hemodynamics. These methods are widely used by the scientific community, but are almost always too complicated for transitional medicine, and even more complicated for wide application in real clinical practice. Long time computer simulations on workstations do not fit into the treatment process, and supercomputer calculations usually do not fit the budget of an average hospital. Free or shareware computing resources (open access supercomputers) are not always available, since they have long queues for computing.

So, it is important to create methods and tools that would combine the already existed risk factor analysis and aneurysm geometry determination with a quick but informative procedure for assessing the form of cerebral vessels from their biomechanical properties [1-3].

II. Methods and Materials

The key features of the suggested method are the following. A series of structural 2D OCT-images (B-scans) of the blood vessel wall under the study or using phantoms is obtained using intravascular OCT system [4]. A first structural OCT-image (Fig. 1a) is selected corresponding to the moment of diastole. This image corresponds to the main, least deformed state of the blood vessel wall under the study. Similarly, the second OCT-image (Fig. 1b) of the investigated blood vessel wall is selected at the time of its systolic expansion. The moments of systole and diastole are to be determined using an blood pressure sensor inserted into the intravascular probe catheter [4, 5]. The value of the deforming effect of the pulse wave is calculated using data of the systolic, P_{SYS}, and diastolic, P_{DIA}, blood pressure, as well as a coefficient, k_{norm}, the normal component of this pressure value.

Significant noise of standard intravascular OCT system complicates the process of quantitative evaluation of blood wall

978-1-7281-8073-1/20/$31.00 ©2020 IEEE

displacement under study [6-8]. The result of addition and averaging of all vessel wall OCT-image A-scans into one (from Fig. 1) is shown in Fig. 2. To increase signal-to-noise ratio (SNR) it is necessary to reduce the AD quantization number of all structural OCT-image. In such a way the SNR is increased by at least one order of magnitude [4]. The value of the blood vessel wall longitudinal displacement, Δl, is calculated from the peak intensity shift of the averaged sum of all A-scans for each analyzed OCT-image.

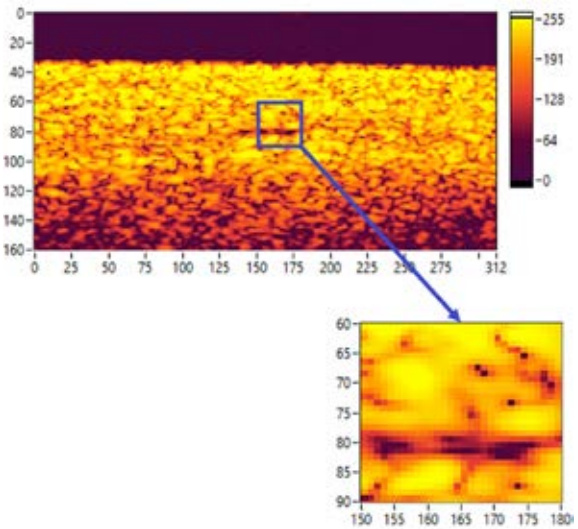

(a)

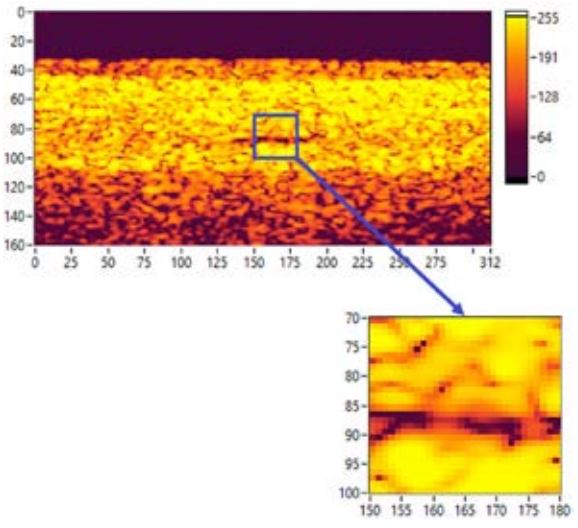

(b)

Fig. 1. B-scans of the wall of phantom of the blood vessel under study in undeformed (a) and deformed (b) situation. Each scan contains 256 levels of quantization.

The area the pulse wave deforming effect is considered to be equal the entire area of the of the blood vessel wall. However, deformations, as well as the value of the deforming force, are monitored in the scanning area of the intravascular OCT probe only [9-11]. Therefore, the area of the deformation, S, of the blood vessel wall is to be equal to the scanning area of the applied intravascular OCT-probe [12, 13]. Equality of the areas allows for truncating them from calculations. Deformations that occur in the blood vessel wall during the pulse wave propagation smoothly fade in the surrounding tissues. However, only deformations within the analyzed OCT-scans are taken into account in the final calculations. Therefore, the depth of visualization by the OCT method (coherence probing depth – CPD) should be equated to the longitudinal dimension, l, *i.e.* thickness of the deformed area.

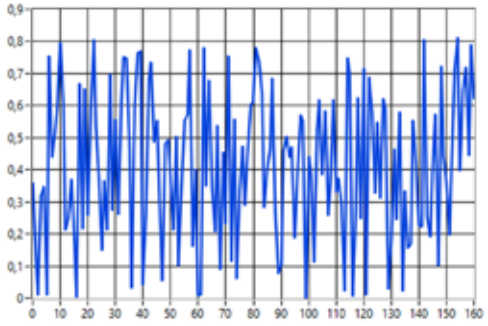

(a)

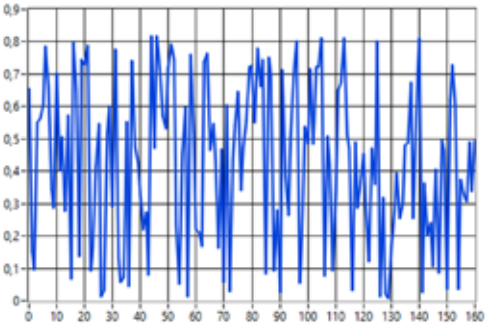

(b)

Fig. 2. A result of the averaging of all A-scans of the undeformed image of the phantom of blood vessel wall (a) and the deformed one (b). The noise makes it difficult to analyze the obtained A-scans.

Young's modulus is calculated using the following formula:

$$E \approx \frac{l \cdot k_{norm} \cdot (P_{SYS} - P_{DIA})}{\Delta l}.$$

Finally, Young's modulus value is shown to the user together with the data of current blood pressure in the part of the blood vessel [4, 13].

III. Results and Discussion

The essential computation of the described method for the Young's modulus evaluation for the cerebral arteries walls with aneurysms was made using dedicated software implemented in the LabVIEW package [4].

Some of the steps in the method are already known and described earlier [8, 14-16]. These are, the area of the intravascular OCT-probe calculation (in our case, $S \approx 8.05$ mm2); CPD calculation for a given type of OCT-system and an

object under the study (in this case, $l \approx 0.78$ mm); a sequence of B-scans acquisition (in this case, 20 B-scans/s); systolic and diastolic blood pressure data recoding (in this case, $P_{SYS} = 20.66$ kPa and $P_{DIA} = 9.33$ kPa), etc. Details of these steps are given elsewhere [4, 16]. The key stage of our algorithm is OCT-image AD re-quantization, only this approach is described here. The same B-scans of the investigated blood vessel as shown in Fig. 1. are Fig. 3., but the number of discretization levels has been reduced from 256 to 6. The original image has 0 to 255 levels (typical for 8-bit images). New image has 6 levels only: 87, 152, 195, 218, 236, 251.

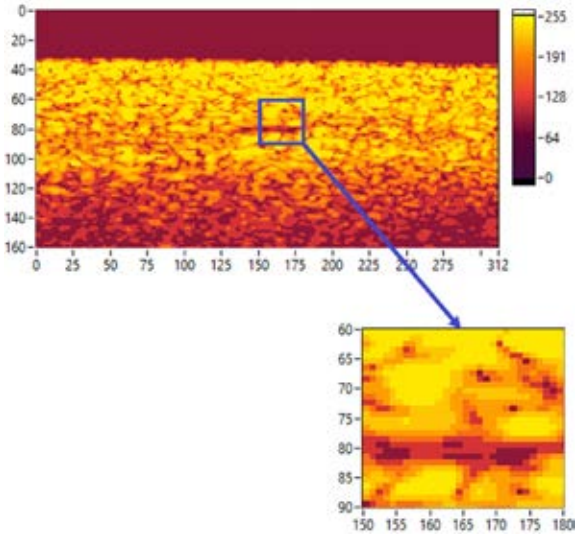

(a)

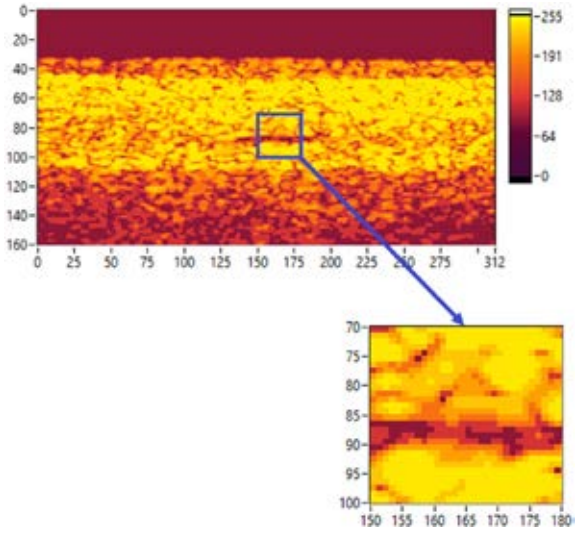

(b)

Fig. 3. B-scans of the wall of the phantom of the blood vessel under the study in undeformed (a) and deformed (b) cases after re-quantization. Each scan contains 6 levels of quantization only.

The new levels have been chosen on purpose, in particular the choice is aimed at a forceful increase in the signal-to-noise ratio, even by losing a part of the useful signal. The histograms of the processed OCT-images were digitally analyzed, the new levels provide equivalent signal intensity in all parts of the image [4]. New levels are selected in such a way that the sums of the products of the number of pixels times their intensities at the intervals are to be equal (taking into account the calculation error). The loss of about 10% of the useful information is the result of the described processing, though the noise component was almost completely removed [13, 17]. After the processing, B-scans visually look worse than the original ones (compare Fig. 3 and Fig. 1), but they are not thought to be demonstrated intermediately. The only purpose of such processing is to have the exact digital data of the averaged A-scans (compare Fig. 4 and Fig. 2). Obvious increase in the SNR makes the calculation a routine problem (Fig. 4). In this case, the displacements of some parts the object under the study could be estimated from the shift of the peak intensities, shifts of a given number of local maxima, shift of test points, etc. [18-20] In the example (Fig. 1 - Fig. 4), the peak intensity shift was 9 pixels, which is equivalent to $\Delta l \approx 70$ microns of absolute displacement of the structures. Young's modulus is calculated using the classical formula, in this case it was calculated as, $E \approx 0.89$ MPa.

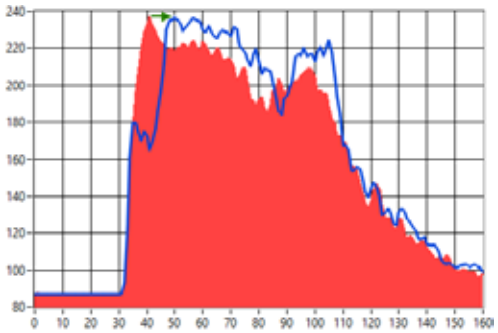

Fig. 4. A result of the averaging of all A-scans of the undeformed image of the phantom of blood vessel wall (red area chart) and the deformed one (blue curve) aftter re-quantization. The green arrow shows the shift of the intensity peak. The noise of the obtained A-scans is considerably reduced.

The prospects for using the proposed method in real clinical practice are advisable to discuss. Surgical deployment of a flow-diverter is always performed through an incision in the femoral artery. The flow-diverter is delivered to the affected cerebral artery with a special guide and is expanded. Control over the deployment of the diverter is carried out using X-rays because any flow-diverter contains a strip of radio-opaque material to simplify the process of spatial positioning. Thus, an incision in the femoral artery is made in any case during the flow-diverter deployment. An intravascular probe of the OCT-system could be inserted through this incision before surgery [4, 13]. This allows for evaluating the biomechanical properties of the walls of the affected artery and the blood pressure in it. It is important to note, that blood vessel walls are too thin structures for ultrasound and magnetic resonance elastography. A biopsy and subsequent laboratory analysis of a fragment of the blood vessel wall is used only for the analysis of atherosclerotic plaque. It is extremely dangerous to expose an aneurysm to biopsy. X-ray angiography allows you to get a lot of useful information about the morphology of blood vessels under study. It is used to control the process of spatial movement of the intravascular

probe for this reason. However, X-ray angiography not allow evaluate of biomechanical properties of blood vessel walls. Thus, the proposed method is not a competitor, but complementary to the above to well-known methods of medical imaging. The efficiency of type selection of a flow-diverter will increase considerably with the new data [21]. If the new nonionizing information indicates that a planned surgery of the flow-diverter deployment is inexpedient or ineffective, it could be canceled or replaced with a similar one (embolization, for example).

IV. Conclusion

A method for evaluating Young's modulus for the walls of the cerebral arteries was described. The key features of the method are: I) application of a pulse wave as a deforming force; II) calculation of the magnitude of the deforming vessel effect considering the difference in the values of systolic and diastolic pressure under the study; III) using of operations of re-quantization of structural OCT-images to obtain clearly distinguishable and stable shapes of averaged A-scans; IV) the CPD consideration as an equivalent of the thickness of the deformable region of the processed B-scans; V) equating the area of the deforming effect to the scanning area of the applied intravascular OCT-probe.

Accuracy of the Young's modulus evaluation by the described method is more than 90%. The calculated value of Young's modulus was $E \approx 0.89$ MPa in the considered case (Fig. 1- Fig. 4). This value is below the norm and indicates insufficient resistance of blood vessel wall under the deforming influence and, therefore, could lead to vessel wall rapture. Note that, intravascular surgery for deployment a flow-diverter can be also performed through the incision used to insert the OCT-probe. Therefore, there is a significant risk of rupture of the blood vessel under study. Further research will be focused on the transition from a evaluation to the quantitative assessment of the probability of blood vessel rupture in relation to long time intervals (one-year, five-year, etc. probabilities) and to the blood pressure differences (evaluation of resistance to sharp pressure changes).

Acknowledgment

This work was supported by the Russian Science Foundation (RSF project 16-15-10327).

References

[1] B.F. Kennedy, K.M. Kennedy and D.D. Sampson, "A Review of Optical Coherence Elastography: Fundamentals, Techniques and Prospects," IEEE Journal of Selected Topics in Quantum Electronics, vol. 20, no. 2, art. no. 7101217, pp. 272-288, April 2014.

[2] J.P. Rolland, F. Zvietcovich, G.R. Ge and K.J. Parker, "Perspectives and advances in optical elastography," Optical Elastography and Tissue Biomechanics - Proceedings of SPIE, vol. 10880, art. no. 108800G, February 2019.

[3] K.V. Larin, "Dynamic Optical Coherence Elastography of Soft Tissue," Proceedings of the IEEE. International Conference Laser Optics (ICLO), art. no. 8435277, pp. 509-509, August 2018.

[4] S.V. Frolov and A.Yu. Potlov, "An Endoscopic Optical Coherence Tomography System with Improved Precision of Probe Positioning," Biomedical Engineering, vol. 53, no. 1, pp. 6-10, May 2019.

[5] B.E. Bouma, M. Villiger, K. Otsuka and W.-Y. Oh, "Intravascular optical coherence tomography," Biomedical Optics Express, vol. 8, is. 5, pp. 2660-2686, April 2017.

[6] A.N. Bashkatov, E.A. Genina, V.I. Kochubey and V.V. Tuchin, "Quantification of tissue optical properties: perspectives for precise optical diagnostics, phototherapy and laser surgery," Journal of Physics D: Applied Physics, vol. 49, no. 50, art. no. 501001, November 2016.

[7] R.W. Kirk, B.F. Kennedy, D.D. Sampson and R.A. McLaughlin, "Near Video-Rate Optical Coherence Elastography by Acceleration With a Graphics Processing Unit," Journal of Lightwave Technology, vol. 33, no. 16, pp. 3481-3485, August 2015.

[8] L. Chin, P. Wijesinghe, B. Latham, C.M. Saunders, D.D. Sampson and B.F. Kennedy, "Mapping the mechanical heterogeneity of human breast tissue using optical coherence elastography," OSA Technical Digest (conference: Cancer Imaging and Therapy), art. no. JM2A.3, January 2016.

[9] X. Liu, B. Hubbi and X. Zhou, "Spatial coordinate corrected motion tracking for optical coherence elastography," Biomedical Optics Express, vol. 10, is. 12, pp. 6160-6171, November 2019.

[10] D.S. Prabhu, H.G. Bezerra, C. Kolluru, Y. Gharaibeh, E. Mehanna, H. Wu and D.L. Wilson, "Automated A-line coronary plaque classification of intravascular optical coherence tomography images using handcrafted features and large datasets," Journal of Biomedical Optics, vol. 24, is. 10, art. no. 106002, October 2019

[11] X. Liang and S.A. Boppart, "Biomechanical Properties of In Vivo Human Skin From Dynamic Optical Coherence Elastography," IEEE Transactions on Biomedical Engineering, vol. 57, no. 4, pp. 953-959, April 2010.

[12] A. Podoleanu, "Advances in Optical Coherence Tomography," Proceedings of the IEEE. 20th International Conference on Transparent Optical Networks (ICTON), art. no. 8473778, pp. 1-4, September 2018.

[13] S.V. Frolov, A.Yu. Potlov, T.A. Frolova and S.G. Proskurin, "Compression elastography and endoscopic optical coherence tomography for biomechanical properties evaluation of cerebral arteries walls with aneurysm and their phantoms," AIP Conference Proceedings, vol. 2140, art. no. 020020, August 2019.

[14] M. Neidhardt, M. Bengs, S. Latus, M. Schlüter, T. Saathoff and A. Schlaefer, "Deep Learning for High Speed Optical Coherence Elastography," Proceedings of the IEEE. 17th International Symposium on Biomedical Imaging (ISBI), art. no. 9098422, pp. 1583-1586, May 2020.

[15] H. Liou, F. Sabba, G. Wells and O. Balogun, "Mechanical Characterization of Biofilms by Optical Coherence Elastography (OCE) Measurements of Elastic Waves," Proceedings of the IEEE. International Ultrasonics Symposium (IUS), art. no. 8925714, pp. 2194-2197, December 2019.

[16] A.Yu. Potlov, S.V. Frolov and S.G. Proskurin, "Visualization of Anatomical Structures of Biological Tissues by Optical Coherence Tomography with Digital Processing of Morphological Data," Biomedical Engineering, vol. 54, no. 1, pp. 9-13, May 2020.

[17] A.N. Bashkatov, E.A. Genina and V.V. Tuchin, "Optical Properties of Skin, Subcutaneous, and Muscle Tissues: a Review," Journal of Innovative Optical Health Sciences, vol. 4, no 1, pp. 9-38, January 2011.

[18] Y. Gharaibeh, D.S. Prabhu, C. Kolluru, J. Lee, V. Zimin, H.G. Bezerra and D.L. Wilson, "Coronary calcification segmentation in intravascular OCT images using deep learning: application to calcification scoring," Journal of Medical Imaging, vol. 6, is. 4, art. no. 045002, December 2019.

[19] A.Yu. Potlov, S.V. Frolov, T.A. Frolova and S.G. Proskurin, "High-precision evaluation of stress-related properties of blood vessel walls using intravascular optical coherence elastography with forward-view probe," Progress in Biomedical Optics and Imaging - Proceedings of SPIE, vol. 11457, art. no. 114571P, April 2020.

[20] J. Li, C.-H. Liu, A. Schill, M. Singh, Y.V. Kistenev, K.V. Larin, "A comparison study of optical coherence elastography and laser Michelson vibrometry," Optical Elastography and Tissue Biomechanics - Proceedings of SPIE, vol. 9710, art. no. 97101A, March 2016.

[21] S.V. Sindeev, S.V. Frolov and A.Yu. Potlov, "Mathematical Modeling of Blood Flow in a Patientspecific Model of the Middle Cerebral Artery Taking into Account Non-Newtonian Blood Behavior," Proceedings of the IEEE. International Science and Technology Conference «EastConf», art. no. 8725318, pp. 1-5, May 2019.